Vibrational Energy Transfer between Carbon Nanotubes and Liquid Water: A Molecular Dynamics Study

Tammie R. Nelson,[†] Vitaly V. Chaban,[‡] Oleg N. Kalugin,[‡] and Oleg V. Prezhdo*,[†]

Department of Chemistry, University of Washington, Seattle, Washington 98195, and Department of Inorganic Chemistry, V. N. Karazin Kharkiv National University, Kharkiv, Ukraine

Received: December 29, 2009; Revised Manuscript Received: February 19, 2010

The rates and magnitudes of vibrational energy transfer between single-wall carbon nanotubes (CNTs) and water are investigated by classical molecular dynamics. The interactions between the CNT and solvent confined inside of the tube, the CNT and solvent surrounding the tube, as well as the solvent inside and outside of the tube are considered for the (11,11), (15,15), and (19,19) armchair CNTs. The vibrational energy transfer exhibits two time scales, subpicosecond and picosecond, of roughly equal importance. Solvent molecules confined within CNTs are more strongly coupled to the tubes than the outside molecules. The energy exchange is facilitated by slow collective motions, including CNT radial breathing modes (RBM). The transfer rate between CNTs and the inside solvent shows strong dependence on the CNT diameter. In smaller tubes, the transfer is faster and the solvent coupling to RBMs is stronger. The magnitude of the CNT−outside solvent interaction scales with the CNT surface area, while that of the CNT−inside solvent exhibits scaling that is intermediate between the CNT volume and surface. The Coulomb interaction between the solvent molecules inside and outside of the CNTs is much weaker than the CNT−solvent interactions. The results indicate that the excitation energy supplied to CNTs in chemical and biological applications is rapidly deposited to the active molecular agents and should remain localized sufficiently long in order to perform the desired function.

1. Introduction

Carbon nanotubes (CNTs) are hollow cylindrical structures formed from sp^2 hybridized carbon atoms arranged in a hexagonal pattern. CNTs can be single-walled or multiwalled with nanometer scale diameters. Since their discovery in 1991,[1] following the unnoticed reports back in 1952,[2] CNTs have received great attention from the scientific community.[3] Their potential use in a variety of devices, such as field effect transistors[4] and solar cells,[5] has captured the interests of a broad range of fields from biological to material sciences.[6] The electronic, vibrational, and optical properties of CNTs form the physical basis for the practical applications and are the focus of extensive studies.[7−12]

The idea of using the hollow cylindrical structure of the CNT as a transporter or container has existed for many years. Recently, it has drawn particular attention from the medical community, with the hope of creating a new delivery device for small therapeutic agents such as proteins, nucleic acids, vaccines, and other biologically active molecules.[13−15] CNTs offer a unique and effective cell-penetrating transporter; previous studies have shown that they are capable of entering mammalian cells while maintaining relatively low toxicity levels.[16,17] CNTs are optically active in the spectral region that is transparent for the biological tissues, creating an excellent possibility for optical control of the therapeutic agent release.[18−20] In addition to the biological applications, encapsulation of molecules, such as fullerenes and a variety of gases, provides a novel chemical reaction environment. A variety of chemical transformations occur inside of CNTs at a substantially lower energy barrier.[21,22]

Applications requiring decoration of the outer tube wall are becoming increasingly prominent as functionalization offers an effective route to fine-tuning the electronic-transport properties[23] and solubility[24] of tubes. Functionalized CNT walls can serve as molecular linkers for the attachment and transport of bioactive molecules, such as proteins and nucleic acids, as well as other small molecules.[25] CNT−DNA complexes,[26] in which DNA is helically wrapped around a nanotube, have gained recent attention for their potential use both in biological delivery systems[13] and with CNT purification and separation.[27]

Our study is motivated by the desire to understand the role of CNTs in the chemical and physical transformations occurring at or in close proximity to their interior and exterior surfaces. In particular, vibrational energy transfer to the interior and exterior of CNTs can initiate reactions inside of tubes and alter electronic properties by reversing functionalization of the outer walls, respectively. Photoexcitation of a biologically functionalized transport CNT can be used as a method for releasing a molecule from inside of the tube or unwrapping a polymer or a DNA strand from the exterior of the tube. In all of these cases, vibrational energy from the tube must dissipate to the tube interior or exterior fast enough and remain localized long enough to provide sufficient energy for the transformation to occur.

Experimental[28−33] and theoretical[34−36] studies show that the optical excitation energy is rapidly equilibrated within a CNT. The electronic energy is deposited into high-frequency vibrational modes within tens to hundreds of femtoseconds,[28−31,35] while the high-frequency phonons equilibrate with the low-frequency modes after about a picosecond.[32,33] The rate of the excitation energy transfer to the surrounding media has received attention only recently.[37,38]

In this paper, we investigate vibrational energy transfer from CNTs to solvating water molecules on the interior and exterior of the tube. Water was chosen as the solvent because of its

* To whom correspondence should be addressed. E-mail: prezhdo@u.washington.edu.
[‡] Kharkiv National University.
[†] University of Washington.

10.1021/jp912233e
Published on Web 03/15/2010

TABLE 1: Details of the Simulated Systems, Including the CNT diameter, d_{tube}, Outer Surface Area, SA_{out}, Inner Surface Area, SA_{in}, Inner Volume, Vol_{in}, Number of Molecules Outside of the Tube, N_{out}, and Number of Molecules Inside of the Tube, N_{in}[a]

CNT	d_{tube}, nm	SA_{out}, nm^2	SA_{in}, nm^2	Vol_{in}, nm^3	N_{out}	N_{in}
(11,11)	1.49	37.6	21.0	5.8	1517	208
(15,15)	2.03	48.5	31.2	12.9	1836	462
(19,19)	2.58	59.5	41.6	22.9	2157	814

[a] All CNTs were 6.4 nm in length. The CNT diameter was defined as the distance between the centers of two opposing carbon atoms. The van der Waals diameter of a carbon atom (0.38 nm) was used to determine the outer and inner CNT diameters.

physiological and chemical relevance. The excess vibrational energy can be deposited into CNTs either directly, with IR radiation or thermally, or indirectly by photoexciting electronic degrees of freedom that rapidly transfer their energy to vibrational modes. We study the time scales and magnitudes of energy dissipation as functions of the CNT diameter, curvature, surface area, and volume. We also investigate vibrational energy transfer between water molecules inside and outside of the tube, facilitated by the long-range Coulomb interaction. We determine whether the energy is partitioned uniformly to the interior and exterior regions of the tube or whether there is a preferred direction for the transfer. Finally, we characterize the phonon modes that are responsible for the energy dissipation.

The next section describes the CNT and water models used for the calculations and presents the calculation methods. The Results section provides a detailed atomistic description of the CNT−solvent vibrational energy exchange and addresses the questions raised in the previous paragraph. The key findings of our study are discussed and summarized in the Discussion and Conclusions section.

2. Theory

The theory section describes first the details of the molecular dynamics (MD) simulation, including the models of the CNT, water, and CNT−water interaction, and then presents the methods used for the data analysis.

2.1. Simulation Details. Classical MD simulations were performed with three CNT−water systems containing (11,11), (15,15), and (19,19) single-walled armchair CNTs of 1.49, 2.03, and 2.58 nm diameters, respectively.[39] We focus on metallic CNTs because in the case of an electronic photoexcitation, all energy rapidly transfers to vibrations. The corresponding process in semiconducting CNTs involves multiple time scales. High-energy electronic excitations of semiconducting CNTs deposit their energy to phonons and decay to the lowest-energy exciton within about 100 fs. However, the lowest exciton can live for a long time, transferring its energy to phonons on a pico- and even a nanosecond time scale. Each tube was 6.4 nm in length, containing 50 carbon atoms in the axial direction. Open-ended CNTs were immersed in liquid water of bulk density (997 kg/m^3) at 298 K and centered in square parallelepiped simulation cells 6.4 nm in length. A cutoff radius equal to 0.9 nm was applied to all interactions. The volumes of the simulation cells were 114.7, 135.6, and 185.6 nm^3, respectively. The simulated CNTs were surrounded by approximately two layers of water molecules, which is sufficient to describe the overwhelming fraction of solvation energy.[40,41] System details are provided in Table 1, which lists the CNT diameter, the inner and outer CNT surface area, the interior CNT volume, and the number of water molecules inside and outside of each tube. The simulations were performed using the GROMACS software package,[42] including several proprietary utilities for initialization and analysis. The MD simulations were performed with a 0.001 ps time step in the *NVT* ensemble using the Nosé−Hoover thermostat[43] with a 0.1 ps relaxation time. The 1000 ps equilibration and 1000 ps data collection runs were performed with each system.

The site−site interactions between all atom pairs in the MD system are given by the sum of the 12−6 Lennard-Jones (LJ) and Coulomb potentials

$$U(r_{ij}) = 4\varepsilon_{ij}\left[\left(\frac{\sigma_{ij}}{r_{ij}}\right)^{12} - \left(\frac{\sigma_{ij}}{r_{ij}}\right)^{6}\right] + \frac{z_i z_j e^2}{4\pi\varepsilon_0 r_{ij}} \quad (1)$$

where ε_{ij} and σ_{ij} are the LJ parameters between sites i and j of distinct molecules, z_i is the partial charge on site i, and r_{ij} is the site−site separation. Cross interactions were obtained using the Lorentz−Berthelot combining rules

$$\varepsilon_{ij} = \sqrt{\varepsilon_{ii}\varepsilon_{jj}} \quad (2)$$

$$\sigma_{ij} = \frac{(\sigma_{ii} + \sigma_{jj})}{2} \quad (3)$$

A shifted force potential was employed for the LJ part of the potential, whereas the switch method was used to calculate the long-range Coulomb part.[44] The CNT−water interactions were treated as purely LJ since the carbon atoms of perfect CNTs are essentially electroneutral. The water−water interactions were treated with both LJ and Coulomb potentials.

The CNTs were fully flexible. The interatomic potentials between the sp^2 carbon centers were developed[45] by fitting the experimental lattice parameters, elastic constants, and phonon frequencies for graphite. The Morse bond stretches were described by $R_b = 1.4114$, $k_b = 720$, and $D_b = 133$. The cosine angle bends were characterized by $\theta_a = 120$, $k_{\theta\theta} = 196.13$, $k_{r\theta} = -72.41$, and $k_{rr} = 68$. The two-fold torsion potential was $V_t = 21.28$. Here, the distances are given in angstroms, the angles are in degrees, the energies are in kcal mol^{-1}, and the force constants are in kcal mol^{-1}, angstrom, and radian units. The van der Waals diameter of a single carbon atom was estimated to be 0.38 nm based on the distance at the minimum of the interaction potential.[46] Water molecules were treated within the well-known single-point charge (SPC) force field model.[47] The system components and an example of a solvated tube are shown in Figure 1.

2.2. Data Analysis. According to the linear response theory, fluctuations in the interaction energy at equilibrium fully characterize the system response to a nonequilibrium perturbation.[40,41] Excitation of a CNT by an optical signal, and the subsequent vibrational energy transfer from the CNT to a solvent, is a nonequilibrium process. Nevertheless, its rate can be obtained from the equilibrium response function for the corresponding interaction potential, provided that the perturbation is not exceedingly large. Using the linear response theory, we determine the time scales, rates, and magnitudes of energy exchange between different parts of the CNT−water systems by computing the corresponding autocorrelation functions (ACFs).

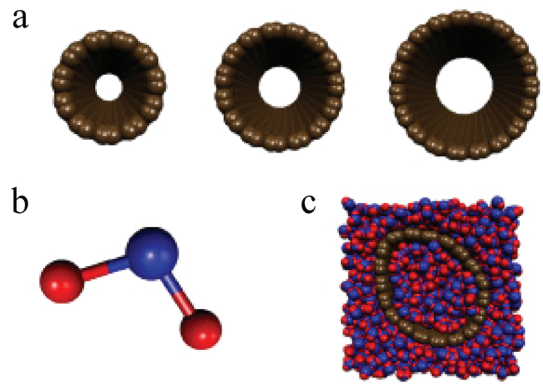

Figure 1. The simulated systems (see Table 1 for system parameters). (a) (11,11), (15,15), and (19,19) single-walled armchair CNTs. (b) Water molecule. (c) (19,19) CNT hydrated at 298 K in a square parallelepiped simulation cell. Each CNT was surrounded by approximately two layers of water molecules.

The normalized ACF $C(t)$ for the relevant interaction energy E is defined as

$$C(t) = \frac{\langle \Delta E(t) \Delta E(0) \rangle}{\langle \Delta E^2(0) \rangle} \tag{4}$$

where the brackets denote statistical ensemble averaging and $\Delta E = E - \langle E \rangle$ indicates deviation of the interaction energy from its average value $\langle E \rangle$. The initial value

$$\tilde{C}(0) = \langle \Delta E^2(0) \rangle \tag{5}$$

of the unnormalized ACF

$$\tilde{C}(t) = \langle \Delta E(t) \Delta E(0) \rangle \tag{6}$$

quantifies the magnitude of the interaction.

The calculated ACFs, eq 4, showed biexponential decay and were fit to the function

$$f(t) = A_{\text{fast}} e^{-t/\tau_{\text{fast}}} + (1 - A_{\text{fast}}) e^{-t/\tau_{\text{slow}}} \tag{7}$$

Here, τ_{fast} and τ_{slow} are the time scale of the fast and slow components of the vibrational energy relaxation, and A_{fast} and $1 - A_{\text{fast}}$ are the corresponding amplitudes. The cosine Fourier transform of the ACF, known as the spectral density,[40,41] was computed for each interaction type and tube size

$$I(\omega) = \int_{-\infty}^{\infty} C(t) \cos(\omega t) dt \tag{8}$$

The intensity I and frequency ω of the spectral density identify the vibrational motions that promote the selected vibrational energy exchange process.

3. Results

The time scales of the vibrational energy exchange between the CNTs and interior and exterior solvent are characterized by the corresponding ACFs, which are shown in Figure 2. The ACFs were computed according to eq 4 for each tube size and interaction type, including the interactions between the CNT and water inside of the tube (CNT−in), the CNT and water outside of the tube (CNT−out), as well as water inside of and water outside of the tube (in−out). The biexponential fits, eq 7, showed fast and slow decay components. Table 2 presents the fitting parameters, including the time scale and amplitude of each component. The fast, ballistic relaxation occurs by direct collisions between the two subsystems.[40,41] The ballistic com-

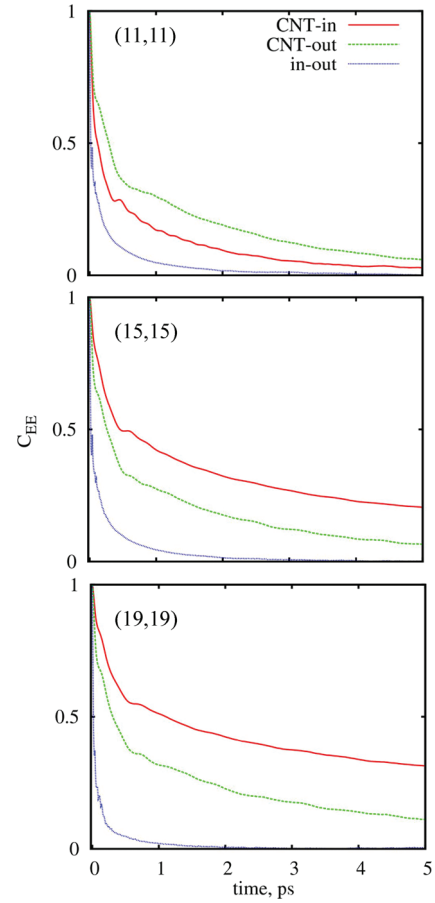

Figure 2. Normalized energy ACFs for the (11,11), (15,15), and (19,19) CNTs (top, middle, and bottom panels, respectively). The CNT−inside interaction is represented by the solid (red) line, the CNT−outside interaction is represented by the dashed (green) line, and the inside−outside Coulomb interaction is represented by the dotted (blue) line. Each ACF comprises fast and slow decay components; see eq 7 and Table 4.

TABLE 2: Biexponential Fitting Parameters (eq 7) of the Normalized ACFs for Each Interaction Type and CNT Size[a]

	A_{fast}	τ_{fast}, ps	τ_{slow}, ps
CNT−In			
(11,11)	0.67	0.09	1.65
(15,15)	0.50	0.21	5.12
(19,19)	0.45	0.24	8.09
CNT−Out			
(11,11)	0.56	0.15	2.41
(15,15)	0.60	0.15	2.55
(19,19)	0.58	0.18	3.53
In−Out			
(11,11)	0.67	0.02	0.48
(15,15)	0.66	0.02	0.44
(19,19)	0.78	0.02	0.33

[a] Decay times, τ, for the fast and slow components are given along with the amplitude, A, for the fast component. The data indicates that over half of the vibrational energy is transferred on a subpicosecond time scale, and the remainder of the energy is dissipated within a few picoseconds.

TABLE 3: Rates, k, of the Fast Component of the CNT−Water Vibrational Energy Transfer Per Molecule of Solvent Inside and Outside of the Tube[a]

CNT	k_{in}, ps^{-1}/molecule	k_{out}, ps^{-1}/molecule
(11,11)	0.053	0.0044
(15,15)	0.010	0.0036
(19,19)	0.005	0.0026

[a] Note that the outside solvent comprises about two solvation shells for all tubes. As the tube size increases, the rate of inside transfer decreases, while the outside transfer rate remains relatively constant.

ponent of vibrational energy transfer between the CNT and water can be described by considering the sum of the binary interactions of the CNT with individual water molecules and ignoring the interactions between water molecules. The slow, diffusive relaxation is due to collective motions within each subsystem. It involves anharmonic coupling between vibrational modes of the tube, as well as long-range interactions between water molecules, leading to their reorientation and displacement. The fast part of the ACF relaxation takes less than a picosecond and accounts for over half of the vibrational energy dissipation. The remainder of the relaxation process takes several picoseconds (Table 2).

The vibrational energy exchange between the CNT and exterior water shows little variation with the CNT diameter. In contrast, the communication between the CNT and interior water is very fast for narrow CNTs and dramatically slows down for larger tubes. Further, the amplitude of the fast component is greater than that of the slow component for the smallest (11,11) CNT. The situation is reversed for the largest (19,19) tube, and the (15,15) CNT shows an intermediate behavior. Note that the order of the CNT−in and CNT−out lines in Figure 2 switches between the (11,11) and (15,15) CNTs. The strong dependence of rate of the CNT−inside energy exchange on the CNT diameter can be rationalized by the extent of the solvent subsystem confined inside of the tube. There are few water molecules inside of the smaller CNT. These molecules interact strongly with the tube, generating a fast response. The collective diffusive solvent response is less significant than the direct ballistic response in this case due to the small size of the water subsystem inside of small tubes. In addition to the stronger CNT−water interaction, the faster CNT−water vibrational energy transfer in narrow CNTs is facilitated by the stiffer, ice-like behavior of confined water.[48−50] The enhanced rigidity of confined water increases coupling between water molecules, helping the molecules to accommodate the CNT excess vibrational energy at a faster rate.

The communication between the interior and exterior parts of the solvent is fast and dominated by the ballistic component. The light and relatively weakly coupled water molecules can rapidly adjust their trajectories in response to the long-range Coulomb forces. However, the magnitude of the coupling between the interior and exterior water is small, as quantified below. Therefore, if a photoexcited CNT creates a disbalance between the local temperatures of the interior and exterior solvent, the weak Coulomb interaction between the two solvent subsystems will not be able to balance the temperatures directly. The interior and exterior parts of the solvent will equilibrate by interacting with the tube.

Since the fast ballistic component of the solvent response is generated by interaction of the CNT with individual water molecules, the corresponding relaxation rate, $1/\tau_{fast}$, is equal to the sum of the rates due to each molecule. Table 3 lists the

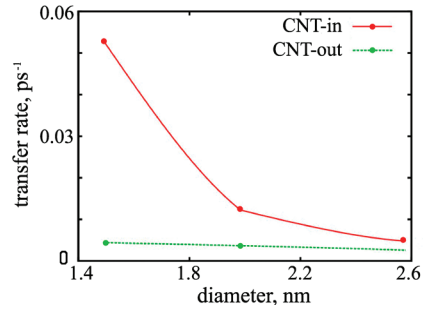

Figure 3. The rates of the CNT−water vibrational energy transfer per water molecule for the inside and outside solvent (Table 3) plotted as functions of the CNT diameter. The rate of vibrational energy transfer from the CNT to the interior of the tube decreases with increasing radius because fewer water−tube interactions are possible. A plateau is reached when the surface becomes planar at the molecular scale. The inner and outer surfaces of the tube appear planar in the infinite size limit, causing both rates to approach the same value.

transfer rates calculated per molecule for the CNT−inside and CNT−outside interactions. The rates are plotted in Figure 3. Since the CNT−molecule interaction depends strongly on the CNT−molecule distance, the interaction per molecule should average to zero for the bulk solvent that extends infinitely far outside of the tube. The outside rates reported in Table 3 make physical sense and can be compared with each other and the inside rates because the outside solvent comprises approximately two solvation shells for all three systems. As the CNT diameter increases, the rate of the CNT−inside energy transfer per molecule decreases, while the CNT−outside transfer rate remains relatively constant. A larger tube has a greater radius of curvature than a smaller tube, causing the surface to appear increasingly planar at the molecular level for larger tubes. The rate of vibrational energy transfer from the CNT to the tube interior decreases with increasing radius because fewer water−tube interactions are made. Both the inner and outer surfaces of the tube appear planar in the infinite size limit. Therefore, the CNT−inside and CNT−outside rates should approach the same value, as seen approximately in Figure 3.

In order to characterize the phonon modes that are responsible for the coupling between the CNTs and water, we computed the spectral densities (eq 8) for the different types of interactions and CNT sizes. The resulting spectra are shown in Figure 4. The intensity is presented in arbitrary units; however, the scales are the same in all plots. The spectra show that the vibrational energy transfer between the CNTs and water is facilitated by low-frequency modes. The highest frequencies are seen in the region from 150 to 250 cm^{-1} that corresponds to CNT radial breathing modes (RBM).[3] An example of the RBM-induced deformation that changes the CNT cross section from circular to ellipsoidal is shown in Figure 1c. As the CNT size increases, the RBM peaks in the spectral density become smaller. This effect is particularly pronounced for the CNT−inside interaction and, to a lesser extent, in the CNT−outside spectra. The inside−outside spectra exhibit little systematic change with CNT size, as expected. The disappearance of the RBM frequencies for the large tubes correlates with the slowing down of the CNT−inside interaction response (Tables 2 and 3). This correlation leads us to conclude that RBMs are particularly important in determining the relaxation time scale. They are the fastest collective motions that create strong CNT−water coupling. Many types of vibrations that have higher frequencies than RBMs exist, for instance, C−C stretches and bends in CNTs, water librations, O−H bends and stretches, and so forth, and these motions are local. The

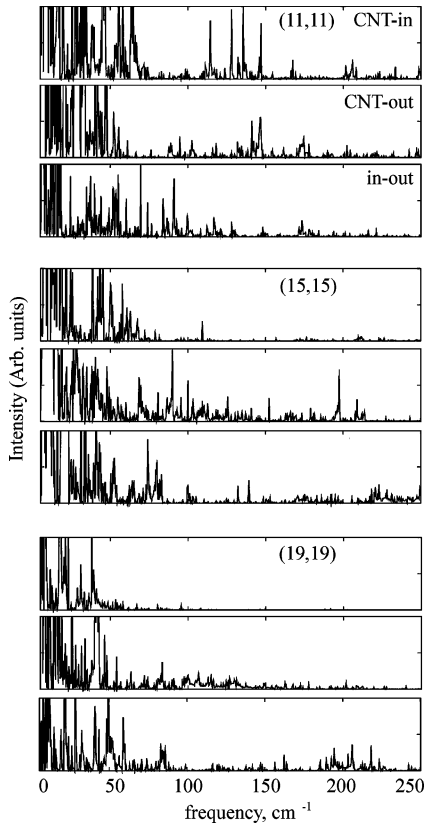

Figure 4. Spectral densities for the CNT−inside, CNT−outside, and inside−outside interactions, produced by Fourier transform of the ACFs (eq 8). The spectral densities characterize the phonon modes that facilitate the interactions. Top, middle, and bottom panels show the spectra for the (11,11), (15,15), and (19,19) CNTs, respectively. The same intensity units are used in all plots. Low-frequency modes dominate the spectra, with the highest frequencies seen in the 150−250 cm^{-1} region corresponding to the CNT RBMs. The disappearance of the RBM frequencies for the larger tube sizes is responsible for the slowing of the CNT−inside transfer rate (Tables 2 and 3).

contribution of the local modes to the large-scale energy flow vanishes when averaged over the whole system.

Finally, we consider the magnitudes of the interactions between the CNTs and water inside and outside of the tubes. The interaction magnitude is well-represented by the average quadratic fluctuation of the interaction energy (eq 5). Coincidentally, this value determines the initial magnitude of the unnormalized ACF (eq 6). The energy fluctuation was computed for each type of interaction and was divided by the number of water molecules involved in the interaction. The results are shown in Table 4. The data reveal that a greater amount of vibrational energy is transferred per molecule to the interior of the tube than to the tube exterior, and relatively little vibrational energy is transferred between the interior and exterior of each tube. Considering the variation with the CNT size, we observe that the trends in the interaction magnitude are opposite from the trends in the relaxation rates (Table 3). The CNT−outside interaction scales with the outside surface area of the CNTs (Table 1). The CNT−inside interaction appears to be more complex as it does not scale linearly with any of the calculated parameters from Table 1. It grows faster than the CNT−inside surface area but slower than the CNT volume. The interaction between the water molecules in the interior and exterior regions of the tube is much weaker than the CNT−water interaction. It scales linearly with the total number of molecules; the average fluctuation per molecule remains constant with increasing system size (Table 4).

TABLE 4: Average Fluctuation of the Interaction Energy Squared (eq 5) Per Molecule for the CNT−Inside, CNT−Outside, and Inside−Outside Interactions[a]

CNT	$\langle(\Delta E)^2\rangle_{in}/N_{in}$ kJ^2/molecule	$\langle(\Delta E)^2\rangle_{out}/N_{out}$ kJ^2/molecule	$\langle(\Delta E)^2\rangle_{in-out}/N_{total}$ kJ^2/molecule
(11,11)	2.12	0.75	0.10
(15,15)	2.98	0.92	0.11
(19,19)	5.79	1.17	0.10

[a] A greater amount of the CNT vibrational energy is dissipated to the interior than exterior of the tube. The inside−outside solvent interaction is weak, and its magnitude scales linearly with the number of molecules near the tube since the Coulomb interaction is long-ranged. The CNT−outside interaction scales with the outside surface area of the CNTs (Table 1). The CNT−inside interaction grows faster than the inside surface area but more slowly than the volume of the CNTs.

4. Discussion and Conclusions

The vibrational energy exchange between CNTs and water occurs on two time scales. Half or more of the energy is transferred faster than a picosecond. This mode of transfer corresponds to the inertial relaxation component that is produced by direct binary collisions of CNTs with individual water molecules. The remainder of the vibrational energy is exchanged within several picoseconds by the diffusive relaxation mechanism that involves collective motions of the solvent and long-term interactions.

Considering the scenario in which the excess energy is deposited into CNTs by optical excitation of the electronic degrees of freedom, one is bound to conclude that the time scale of the electronic energy relaxation within CNTs overlaps with that for the vibrational energy exchange between CNTs and water. While the electronic energy is deposited into high-frequency phonon modes within 100 fs,[28−30,35] the coupling of these optical phonons with the slower acoustic RBMs requires on the order of a picosecond.[32,33] This falls within the range of the CNT−water relaxation times. Water is a fast solvent, and it is likely that the vibrational energy exchange between CNTs and other, for example, organic, solvents as well as polymers and DNA matrixes proceeds more slowly and is well-separated from the internal CNT relaxation processes.

The coupling between CNTs and water is facilitated by low-frequency collective motions of the two subsystems, including CNT RBMs. The role of RBMs is particularly pronounced in the vibrational energy exchange between the CNTs and the inside water. With increasing tube size, the RBM intensity in the influence spectra decreases, and the CNT−inside transfer slows down. Faster local motions of the CNT and the solvent, such as C−C and O−H stretches and bends, contribute little to the vibrational energy exchange.

The dissipated vibrational energy does not partition equally between the inside and outside regions of the tube. Solvent molecules confined within CNTs couple to the nanotubes more strongly than the outside molecules. The inside solvent molecules are able to interact with a larger number of carbon atoms due to the nanotube curvature. Additional contribution to the stronger coupling with the water molecules inside of the tube can be provided by the enhanced rigidity of confined water, which behaves more ice-like compared to bulk.[48−50] The direct Coulomb interaction between the water molecules in the inside and outside regions is much weaker than the CNT−water interaction. Therefore, the disbalance in the local solvent temperature created by the difference in the vibrational energy transfer to the inside and outside regions is unlikely to disappear

solely due to the long-range interactions within the solvent. The equilibrium will be reached with participation of the CNT.

The reported results have been obtained under two important assumptions. First, the linear response theory was used, providing great computational advantages compared to a direct nonequilibrium simulation.[40,41] The linear response theory is accurate with weak perturbations, that is, if the amount of optical energy deposited into the CNT is not large. In the future, it will be important to establish how much energy can be deposited into the tube before the linear response breaks down. It is possible that the biological and chemical applications involving CNT heating by lasers will require high optical power in order to achieve rapid biological or chemical response. The validity of the linear response assumption in these situations should be tested by nonequilibrium simulations. Second, the interaction between water and CNTs was described by the LJ potential. It was assumed that carbon atoms remain electroneutral. This is an accurate approximation for ideal CNTs in vacuum. However, its validity can be questioned in the presence of highly polar water molecules. The π-electron system of CNTs is quite mobile and can be polarized by external electric fields. It remains to be seen whether fluctuations in the structure of liquid water are strongly coupled to the π-electron polarization. Such studies will require either a new polarizable model of CNTs or an explicit calculation of the CNT electronic structure in the presence of water.

In summary, the vibrational energy exchange between the CNT and water occurs on two time scales. Over half of the transfer occurs within less than a picosecond, and the remaining half requires several picoseconds. The confined water molecules are more strongly coupled to CNTs than the solvent in the outside region. The vibrational energy exchange is facilitated by low-frequency collective phonons, including CNT RBMs. The magnitude and rate of the vibrational energy transfer are intimately linked to the CNT diameter, allowing the energetic environment within and around the CNT to be selected and fine-tuned to meet requirements of specific biological and chemical reactions.

Acknowledgment. The research was supported by grants from NSF CHE-0957280 and ACS PRF 41436-AC6.

References and Notes

(1) Iijima, S. *Nature* **1991**, *354*, 56.
(2) Radushkevich, L. V.; Lukyanovich, V. M. *Russ. J. Phys. Chem.* **1952**, *26*, 88.
(3) Dresselhaus, M. S.; Dresselhaus, G.; Avouris, P. *Carbon Nanotubes: Synthesis, Structure, Properties, and Applications*; Springer-Verlag: Berlin, Germany, 2001.
(4) Javey, A.; Guo, J.; Wang, Q.; Lundstrom, M.; Dai, H. *Nature* **2003**, *424*, 654.
(5) Kongkanand, A.; Dominguez, R. M.; Kamat, P. V. *Nano Lett.* **2007**, *7*, 676.
(6) Baughman, R. H.; Zakhidov, A. A.; de Heer, W. A. *Science* **2002**, *297*, 787.
(7) Bockrath, M.; Cobden, D. H.; Lu, J.; Rinzler, A. G.; Smalley, R. E.; Balents, L.; McEuen, P. L. *Nature* **1999**, *397*, 598.
(8) Yamamoto, T.; Watanabe, S.; Watanabe, K. *Phys. Rev. Lett.* **2004**, *92*, 075502.
(9) Wang, F.; Sfeir, M. Y.; Huang, L. M.; Huang, X. M. H.; Wu, Y.; Kim, J. H.; Hone, J.; O'Brien, S.; Brus, L. E.; Heinz, T. F. *Phys. Rev. Lett.* **2006**, *96*, 167401.
(10) Habenicht, B. F.; Kamisaka, H.; Yamashita, K.; Prezhdo, O. V. *Nano Lett.* **2007**, *7*, 3260.
(11) Kilina, S.; Badaeva, E.; Piryatinski, A.; Tretiak, S.; Saxena, A.; Bishop, A. R. *Phys. Chem. Chem. Phys.* **2009**, *11*, 4113.
(12) Lueer, L.; Hoseinkhani, S.; Polli, D.; Crochet, J.; Hertel, T.; Lanzani, G. *Nat. Phys.* **2009**, *5*, 54.
(13) Bianco, A.; Kostarelos, K.; Prato, M. *Curr. Opin. Chem. Biol.* **2005**, *9*, 674.
(14) Hillebrenner, H.; Buyukserin, F.; Stewart, J. D.; Martin, C. R. *Nanomedicine* **2006**, *1*, 39.
(15) Hampel, S.; Kunze, D.; Haase, D.; Kramer, K.; Rauschenbach, M.; Ritschel, M.; Leonhardt, A.; Thomas, J.; Oswald, S.; Hoffmann, V.; Buchner, B. *Nanomedicine* **2008**, *3*, 175.
(16) Kam, N. W. S.; Jessop, T. C.; Wender, P. A.; Dai, H. *J. Am. Chem. Soc.* **2004**, *126*, 6850.
(17) Pantarotto, D.; Briand, J.; Prato, M.; Bianco, A. *Chem. Commun.* **2004**, 16.
(18) Ghosh, S.; Dutta, S.; Gomes, E.; Carroll, D.; D'Agostino, R., Jr.; Olson, J.; Guthold, M.; Gmeiner, W. H. *ACS Nano* **2009**, *3*, 2667.
(19) Levi-Polyachenko, N. H.; Merkel, E. J.; Jones, B. T.; Carroll, D. L.; Stewart, J. H. *Mol. Pharm.* **2009**, *6*, 1092.
(20) Leach, K. E.; Pedrosa, H. N.; Carlson, L. J.; Krauss, T. D. *Chem. Mater.* **2009**, *21*, 436.
(21) Fujita, Y.; Brandow, S.; Iijima, S. *Chem. Phys. Lett.* **2005**, *413*, 410.
(22) Halls, M. D.; Raghavachari, K. *Nano Lett.* **2005**, *5*, 1861.
(23) Zhao, Y. L.; Stoddart, J. F. *Acc. Chem. Res.* **2009**, *42*, 1161.
(24) Dyke, C. A.; Tour, J. M. *Chemistry* **2004**, *10*, 812.
(25) Campidelli, S.; Klumpp, C.; Bianco, A.; Prato, M. *J. Phys. Org. Chem.* **2006**, *19*, 531.
(26) Yarotski, D. A.; Kilina, S. V.; Talin, A. A.; Tretiak, S.; Prezhdo, O. V.; Balatsky, A. V.; Taylor, A. J. *Nano Lett.* **2009**, *9*, 12.
(27) Enyashin, A. N.; Gemming, S.; Seifert, G. *Nanotechnology* **2007**, *18*, 1.
(28) Hertel, T.; Moos, G. *Phys. Rev. Lett.* **2000**, *84*, 5002.
(29) Manzoni, C.; Gambetta, A.; Menna, E.; Meneghetti, M.; Lanzani, G.; Cerullo, G. *Phys. Rev. Lett.* **2005**, *94*, 207401.
(30) Carlson, L. J.; Krauss, T. D. *Acc. Chem. Res.* **2008**, *41*, 235.
(31) Lueer, L.; Gadermaier, C.; Crochet, J.; Hertel, T.; Brida, D.; Lanzani, G. *Phys. Rev. Lett.* **2009**, *102*, 127401.
(32) Song, D.; Wang, F.; Dukovic, G.; Zheng, M.; Semke, E. D.; Brus, L. E.; Heinz, T. F. *Phys. Rev. Lett.* **2008**, *100*, 225503.
(33) Kang, K.; Ozel, T.; Cahill, D. G.; Shim, M. *Nano Lett.* **2008**, *8*, 4642.
(34) Habenicht, B. F.; Prezhdo, O. V. *Phys. Rev. Lett.* **2008**, *100*, 197402.
(35) Habenicht, B. F.; Craig, C. F.; Prezhdo, O. V. *Phys. Rev. Lett.* **2006**, *96*, 187401.
(36) Perebeinos, V.; Avouris, P. *Phys. Rev. Lett.* **2008**, *101*, 057401.
(37) Perebeinos, V.; Rotkin, S. V.; Petrov, A. G.; Avouris, P. *Nano Lett.* **2009**, *9*, 312.
(38) Rotkin, S. V.; Perebeinos, V.; Petrov, A. G.; Avouris, P. *Nano Lett.* **2009**, *9*, 1850.
(39) Radovic, L. R.; Thrower, P. A. *Chemistry and Physics of Carbon*; Marcel Dekker, Inc.: New York, 2003; Vol. 28.
(40) Prezhdo, O. V.; Rossky, P. J. *J. Phys. Chem.* **1996**, *100*, 17094.
(41) Brooksby, C.; Prezhdo, O. V.; Reid, P. J. *J. Chem. Phys.* **2003**, *119*, 9111.
(42) Hess, B.; Kutzner, C.; Spoel, D. V. D.; Lindahl, R. *J. Chem. Theory Comput.* **2008**, *4*, 435.
(43) Nose, S. *J. Phys.: Condens. Matter* **1990**, *2*, 115.
(44) Steinbach, P. J.; Brooks, B. R. *J. Comput. Chem.* **2004**, *15*, 667.
(45) Guo, Y.; Karasawa, N.; Goddard, W. A. *Nature* **1991**, *351*, 464.
(46) Li, L. J.; Khlobystov, A. N.; Wiltshire, J. G.; Briggs, G. A. D.; Nicholas, R. J. *Nat. Mater.* **2005**, *4*, 481.
(47) Robinson, G. W.; Zhu, S. B.; Singh, S.; Evans, M. W. *Water in Biology, Chemistry, and Physics: Experimental Overviews and Computational Methodologies*; World Scientific: Singapore, 1996.
(48) Mashl, R. J.; Joseph, S.; Aluru, N. R.; Jakobssen, E. *Nano Lett.* **2003**, *3*, 589.
(49) Kalugin, O. N.; Chaban, V. V.; Loskutov, V. V.; Prezhdo, O. V. *Nano Lett.* **2008**, *8*, 2126.
(50) Wang, L.; Zhao, J.; Li, F.; Fang, H.; Lu, J. P. *J. Phys. Chem. C* **2009**, *113*, 5368.

JP912233E